Local-density functional calculations of the energy of atoms

Svetlana Kotochigova, Zachary H. Levine, Eric L. Shirley

M. D. Stiles, and Charles W. Clark

National Institute of Standards and Technology, Gaithersburg, MD, 20899

(January 22, 1997)

Abstract

The total energies of atoms and with atomic number Z from 1 to 92 and singly-charge cations with Z from 2 to 92 have been calculated to an accuracy of 1 μHartree within four variants of the Kohn-Sham local-density approximation. The approximations considered are: the local-density approximation, the local-spin-density approximation, the relativistic local-density approximation, and the scalar-relativistic local-density approximation. The total energies for the LDA are found to be in 0.1% agreement with a large-atomic-number expansion from many-body theory for $Z \geq 40$. Comparison to experiment is made for the ionization energies and spin-orbit splittings; also the total energies and eigenvalues of the various theories are compared among themselves.

I. INTRODUCTION

The Kohn-Sham local-density approximation (LDA) and its variants are widely used in *ab initio* computations of materials properties [14]. This approximation has a demonstrated ability to produce results that, as regards predictive value for ground-state electronic structure, are frequently competitive with the best methods of quantum chemistry. In addition, they have superior scaling properties [1], and so can be applied to much larger systems.

As density-functional approaches become more widespread, there will be a need for benchmark data comparable to those which are available for traditional quantum chemistry. Those who are attempting to solve very large problems, utilizing a range of approximations, will want to distinguish the uncertainties that derive from numerical implementation from those that are inherent in the basic formalism. We have therefore initiated a project to generate reference data that describes results obtained in well-defined, standard approximations with certified numerical accuracy.

There does not appear to have been a comparable effort for LDA in the past. In 1963, Herman and Skillman published self-consistent field solutions across the period table [12], using recognizably modern techniques (i.e., computers programmed with Fortran) capping an effort which had been pursued since the early days of quantum mechanics, particularly by Hartree [11]. Herman and Skillman used an early local-density theory due to Slater [31] which was introduced as an approximate Hartree-Fock theory. In the spirit of the Hartree-Fock, an attractive $1/r$ tail was introduced at large radius to account for exchange in the low-density limit [18]. Shortly thereafter, these results were extended to relativistic systems using the same nonrelativistic exchange-correlation functional [20]. Relativistic functionals were only to become available in the next decade [22,27,28]. Also in the 1970's, spin-polarization was introduced to local-density functional theory [34].

Various surveys of LDA results for large parts of the periodic table have appeared to test various approximations. For example, pseudopotentials for the LDA were presented for atomic numbers Z=1-94, which required the calculation of the corresponding all-electron

atoms [2]. To examine the range validity of pseudopotentials in quantum Monte Carlo calculations, atoms with a single valence electron for Z=1-94 were considered within the non-relativistic local-density approximation [9]. Binding energies of atoms with Z=1-40 for the generalized GW approximation have been compared with those of the LDA and Hartree-Fock [30]. A comparison of some twelve different density functional approximations including gradient-corrected functionals, self-interaction corrections, and nonlocal density functionals was presented for light elements Z=1-18 [7]. While most of the interest of researchers has centered on advances in density functional theory, there does not seem to have been a recent effort to present a complete and comprehensive survey of the electronic structure of atoms within the local density approximation in over three decades [12].

In this article, we present a sample of our results and figures summarizing the results for Z=1-92. Extensive tables of total energies and eigenvalues in four approximations are now available on the World Wide Web [17]. Numerical data presented in this paper is in the usual system of atomic units, in which the mass m and charge e of the electron, and the reduced Planck's constant $\hbar$, take the numerical value of 1. The unit of energy in this system is the Hartree. We calculate the total energies and orbital energy eigenvalues for the ground state configurations of all atoms and singly-charged cations with atomic number $Z \leq 92$ in four standard approximations: (1) The local density approximation (LDA), (2) the local spin density approximation (LSD), (3) the relativistic local density approximation (RLDA), and (4) the scalar-relativistic local-density approximation (ScRLDA). The exchange-correlation energy functional of Vosko, Wilk and Nusair [35] (VWN) is used, with relativistic corrections due to MacDonald and Vosko [22]. There are, of course, a great number of available local-density functionals, including those of Perdew and Wang, [26] Perdew and Zunger, [25] Gunnarsson and Lundqvist, [10] Kohn and Sham, [16] Slater [31] and Wigner. [33] Our purpose here is to create highly precise benchmarks results for one commonly used functional rather than to compare results among the available local-density functionals. In this study, we obtained previously existing codes, and modified them to implement the same density functional, improve numerical accuracy, and regularize input and output. One code

was originally written as a Hartree-Fock atomic structure program, and so required more substantial modifications.

The results presented here derive from four codes, written independently and extensively compared and tested. These were found to give results of good mutual consistency, provided that the numerical approximations within each code were varied until a very high degree of convergence was obtained within each code. One of the authors ran three of the codes, and another ran the fourth to minimize the chance of an input error automatically propagating to all the codes. The authors of the four codes are Sverre Froyen, Donald Hamann, Eric Shirley, and Ilia Tupitsyn and Svetlana Kotochigova. Our target for the precision of the calculation was 1 μHartree in the total energy. We have managed to attain consistency between the independent results at a level that allows us to quote the absolute accuracy for the total energies presented here as 1 μHartree.

II. PROCEDURE

All calculations are all carried out in the framework of generalized Kohn-Sham [16] theory. We use the central field approximation. We limit our calculations to the ground electronic configurations of the first 92 neutral atoms and singly-charged cations of the periodic table. In cases of partially filled electronic subshells, fractional occupancies are assigned to orbitals with different azimuthal quantum number m to accomplish a spherical averaging of the charge distribution. In the case of RLDA, this extends to population-weighted averaging over subshells with the same orbital angular momentum ℓ but different values of total angular momentum j. This choice maximizes the agreement with the ScRLDA calculation which makes the same assumption.

In the LDA, one solves the Kohn-Sham equations

$$[-\frac{1}{2}\nabla^2 + v(\vec{r})]\psi_i(\vec{r}) = \epsilon_i\psi_i(\vec{r}),$$

with

$$v(\vec{r}) = v_{ext}(\vec{r}) + \int d\vec{r}' \frac{\rho(\vec{r})}{|\vec{r} - \vec{r}'|} + v_{xc}(\vec{r}).$$

The charge density ρ is given by

$$\rho(\vec{r}) = \sum_i |\psi_i(\vec{r})|^2,$$

where the sum is over the occupied orbitals indexed by i. The external potential, $v_{ext}(\vec{r})$ is due to the nucleus in the atomic case, i.e., it is $v_{nuc} = -Z/r$. The exchange-correlation potential, $v_{xc}(\vec{r})$, is a function only of the charge density, i.e., $v_{xc}(\vec{r}) = v_{xc}(\rho(\vec{r}))$. For the LSD, a spin-degree of freedom is included [34]; we consider only collinear spin polarization (i.e., the spin is polarized only on the z-axis).

The various parts of the total energy are given by:

$$T = -\frac{1}{2} \sum_i \int d\vec{r} \psi_i^*(\vec{r}) \nabla^2 \psi_i(\vec{r}),$$

$$E_{enuc} = \int d\vec{r} \rho(\vec{r}) v_{nuc}(\vec{r}),$$

$$E_{coul} = \frac{1}{2} \int d\vec{r} d\vec{r}' \frac{\rho(\vec{r})\rho(\vec{r}')}{|\vec{r} - \vec{r}'|},$$

and

$$E_{xc} = \int d\vec{r} \rho(\vec{r}) \varepsilon_{xc}(\rho),$$

where $\varepsilon_{xc}(\rho)$ is the exchange-correlation energy per particle for the uniform electron gas of density ρ; T is the kinetic energy, E_{enuc} is the electron-nucleus energy, E_{coul} is the self-interaction of the charge density viewed as a classical continuum, and E_{xc} is the exchange-correlation energy. This approximation for E_{xc} is the principal approximation of the LDA. In the LSD, these formulas apply with a separate accumulation of the charges with up and down spins.

The relativistic local-density approximation [28] (RLDA) may be obtained from the (nonrelativistic) local-density approximation (LDA) by substituting the relativistic kinetic

energy operator $-i\hbar c\vec{\alpha}\cdot\vec{\nabla}$ for its nonrelativistic counterpart $-\frac{1}{2}\nabla^2$ and using relativistic corrections to the local-density functional. In practice, for the RLDA (and the scalar-relativistic local-density approximation or ScRLDA) the kinetic energy is obtained from

$$T = \sum_i \epsilon_i - \int d\vec{r}\rho(\vec{r})v(\vec{r}).$$

The relativistic wave functions are given by a four-component Dirac spinor at each point in space. The radial equations which are solved by our codes are

$$\frac{dF}{dr} - \frac{\kappa}{r}F = -\alpha(\epsilon - v(r))G,$$
$$\frac{dG}{dr} + \frac{\kappa}{r}G = \alpha(\epsilon - v(r) + 2\alpha^{-2})F,$$

where ϵ is the eigenvalue in Hartrees, and α is the fine structure constant; $\epsilon = 0$ describes a free electron with zero kinetic energy. The functions $G(r)$ and $F(r)$ are related to the Dirac spinor by

$$\psi = \begin{pmatrix} G(r)r^{-1}\mathcal{Y}_{\kappa m}(\hat{r}) \\ iF(r)r^{-1}\mathcal{Y}_{-\kappa m}(\hat{r}) \end{pmatrix}$$

where $\mathcal{Y}_{\kappa m}(\hat{r})$ is a (2-component) Pauli spinor [3].

Dirac's κ quantum number, along with the azimuthal quantum number m, determines the angular dependence of a state. Of the values used in this work, $\kappa = -1, -2, -3$ and -4 correspond to $s_{1/2}$, $p_{3/2}$, $d_{5/2}$, and $f_{7/2}$ states; and $\kappa = 1, 2$ and 3 correspond to $p_{1/2}$, $d_{3/2}$, and $f_{5/2}$ states, respectively. The charge density is obtained from $\rho(\vec{r}) = \sum_\mu |\psi_\mu(\vec{r})|^2$ where μ runs over the four components of the Dirac spinor.

The scalar relativistic approximation is often used for moderately heavy atoms to describe some of the effects of relativity without increasing the number of degrees of freedom. Specifically, it is possible to neglect the spin-orbit splitting while including other relativistic effects, such as the mass-velocity term, the Darwin shift, and (approximately) the contribution of the minor component to the charge density.

Koelling and Harmon [15] have proposed a method to achieve this end, which we call the scalar relativistic local density approximation (ScRLDA). This is a simplified version of the RLDA. The equations to solve are:

$$\frac{d^2G}{dr^2} - \frac{\ell(\ell+1)}{r^2}G = 2M(v(r) - \epsilon)G + \frac{1}{M}\frac{dM}{dr}\left(\frac{dG}{dr} + \frac{\langle\kappa\rangle}{r}\right),$$

where $\langle\kappa\rangle = -1$ is the degeneracy-weighted average value of the Dirac's κ for the two spin-orbit-split levels, and ϵ is the eigenvalue in Hartrees, with the same meaning as in the RLDA.

The parameter M is given by

$$M = 1 + \frac{\alpha^2}{2}(\epsilon - v(r)),$$

where α is the fine structure constant. The charge density is related to G by the formula,

$$r^2\rho(r) = G(r)^2 + \frac{1}{(2Mc)^2}\left[G'(r)^2 + \frac{\ell(\ell+1)}{r^2}G(r)\right]$$

where the contribution due to the minor component is given by the second and third terms.

A. The local density functional

The local density approximation (LDA) requires that the exchange-correlation potential be given as a function of the electron density at a given point in space. The local-spin density approximation (LSD) is similar, with the exchange-correlation potential being given as a function of two variables, the density of up- and down-spin electrons at a given point in space. For atoms, the spin-polarization direction is a constant throughout the atom, which simplifies the formalism. For our study, we use the form of the exchange-correlation potential given by Vosko, Wilk, and Nusair [35]. The form is a fit to the Ceperley-Alder electron gas study [4]. The VWN functional reproduces the random phase approximation (RPA) results for a uniform electron gas in the high density limit, it reproduces the spin-stiffness constant calculated in the RPA in the paramagnetic limit of a uniform electron gas, and it is uniformly differentiable as a function of the electron density. It is also in standard

use, or available as an option, in many electronic structure codes, and thereby provides a convenient reference potential for checking the accuracy of numerical calculations.

The exchange term, as calculated in the RPA, is given by

$$\varepsilon_x(r_s, \zeta) = \varepsilon_x^P(r_s) + [\varepsilon_x^F(r_s) - \varepsilon_x^P(r_s)]f(\zeta). \tag{1}$$

The electron gas parameter r_s, the spin polarization ζ, and the ferromagnetic and paramagnetic exchange energies, $\varepsilon_x^F(r_s)$ and $\varepsilon_x^P(r_s)$ are defined as

$$r_s = \left(\frac{3}{4\pi n}\right)^{1/3},$$

$$\zeta = (n_\uparrow - n_\downarrow)/n,$$

$$\varepsilon_x^P(r_s) = 2^{-1/3}\varepsilon_x^F(r_s) = -3\left(\frac{9}{32\pi^2}\right)^{1/3} r_s^{-1},$$

and $f(\zeta)$ is given by

$$f(\zeta) = \frac{(1+\zeta)^{4/3} + (1-\zeta)^{4/3} - 2}{2(2^{1/3} - 1)};$$

where n is the electron number density (implicitly a function of the spatial coordinates), and $n_\uparrow$ and $n_\downarrow$ its corresponding spin-up and spin-down components ($n = n_\uparrow + n_\downarrow$). Note that $f(0) = 0$ and $f(1) = 1$.

The correlation energy is given by

$$\varepsilon_c(r_s, \zeta) = (1 - f(\zeta)\zeta^4)\varepsilon_c^P(r_s) - f(\zeta)(1 - \zeta^4)\frac{\alpha_c(r_s)}{f''(0)} + f(\zeta)\zeta^4\varepsilon_c^F(r_s).$$

The polarization interpolation, which is more complicated than the interpolation used for the exchange in Eq. (1), obtains the RPA results for the spin stiffness in the paramagnetic limit. $\varepsilon_c^P(r_s) = F(r_s; A, x_0, b, c)$ with the four parameters taken from the "Paramagnetic" line in Table I. (Similar definitions hold for ε_c^F and α_c.) The function F is given by

$$F(r_s; A, x_0, b, c) = A\Big\{ \ln\frac{x^2}{X(x)} + \frac{2b}{Q}\tan^{-1}\frac{Q}{2x+b}$$
$$- \frac{bx_0}{X(x_0)}\Big[\ln\frac{(x - x_0)^2}{X(x)} + \frac{2(b + 2x_0)}{Q}\tan^{-1}\frac{Q}{2x+b}\Big]\Big\},$$

where we have $x = r_s^{1/2}$, $X(x) = x^2 + bx + c$, $Q = (4c - b^2)^{1/2}$. The parameters x_0, b, and c, given in Table I, are used to create three instances of F.

The exchange-correlation potential is given by

$$V_{xc}(n) = \frac{d[n(\varepsilon_x + \varepsilon_c)]}{dn}.$$

We use this form in all of the codes in this study. To avoid errors in the codes, the associated subroutine was recoded independently for one of the codes, although the other three codes shared a common subroutine.

For the RLDA and ScRLDA, we use the correction to the exchange proposed by Mac-Donald and Vosko [22]. (An alternative functional would give similar results [28].) They sought to include, in an approximate way, corrections to the static Coulomb interaction such as the retardation of the Coulomb interaction and the magnetic interaction between moving electrons. In their scheme, the exchange energy is partitioned as

$$E_{xc}[n] = E_x^{DF}[n] + E_x^T[n] + E_c[n],$$

where n is the number density of electrons. Here, DF refers to the "Dirac-Fock" model; T is for "transverse" and represents the terms which are first order in the fine structure constant α. We did not consider relativistic corrections to the correlation [29].

Their corrections are multiplicative, i.e.,

$$\varepsilon_x^{DF}(n) = \varepsilon(n)\phi_C(n)$$

and

$$\varepsilon_x^T(n) = \varepsilon(n)\phi_T(n),$$

where $\varepsilon(\rho)$ is the non-relativistic exchange energy density. Only the sum,

$$\phi_C(n) + \phi_T(n) = \left[1 - \frac{3}{2}\left(\frac{\beta\eta - \ln(\beta + \eta)}{\beta^2}\right)^2\right],$$

with $\beta = v_F/c = (\hbar/(mc))(3\pi^2 n)^{1/3}$ and $\eta = (1 + \beta^2)^{1/2}$, enters into the final formula

$$\varepsilon_{xc}[n] = \varepsilon(n)[\phi_C(n) + \phi_T(n)] + \varepsilon_c[n].$$

(The Fermi velocity is denoted v_F.) At large density, the sign of the correction is negative, i.e., the exchange potential becomes repulsive.

B. Radial grids

Suitable choice of a radial grid is key to obtaining accurate numerical solutions of the integro-differential equations of density-functional theory. The codes make different choices for the radial grid. Two codes make perhaps the simplest choice, an exponentially increasing grid

$$r_n = r_{min} \left(\frac{r_{max}}{r_{min}} \right)^{n/N}$$

with three parameters: the minimum radius, r_{min}, the maximum radius, r_{max}, and the number of intervals, N. The application of the exponential grid to the atomic Schrödinger equation has been discussed by Desclaux [6]. For one code we used $N = 15788$, $r_{min} = 1/(160Z)$, and $r_{max} = 50$. (All distances are in units of the Bohr radius.) Another code used $N \leq 8000$, $r_{min} = 10^{-6}/Z$, and $r_{max} = 800Z^{-1/2}$; in this case, the energies were extrapolated to $n \to \infty$ using an N^{-2} or N^{-4} dependence of the error resulting from finite N, depending on the quantity in question.

Another code involved a grid which was nearly linear near the origin, and exponentially increasing at large r,

$$r_n = a(e^{b(n-1)} - 1),$$

which is determined by three parameters, a, b, and N. This grid includes the origin explicitly as r_1. In this case, we took $a = 4.34 \ 10^{-6}/Z$, $b = 0.002304$, and $r_{max} = 50$, leading to $N = 7058$ for H, increasing to $N = 9021$ for U, and to $r_1 = 10^{-7}$ for H, decreasing to $1.1 \ 10^{-9}$ for U.

A fourth code involved the change of variable

$$\rho = \ln r.$$

A uniform grid is taken in the transformed variable from $\rho(r_{min})$ to $\rho(r_{max})$ where the parameters are taken to be $r_{min} = 0.01e^{-4}/Z$, for atomic number Z, and $r_{max} = 50$. The number of points increased from $N = 2113$ for H to $N = 2837$ for U. The density of points chosen in the latter two codes — linear near the origin and exponentially increasing at large r — is similar to that suggested from theoretical considerations [19].

III. RESULTS

The codes had different functionality, and so different subsets were used to treat each case. Ultimately, we used 4 codes for the LDA results, 3 for LSD, 3 for RLDA, and 2 for ScRLDA.

One goal of this study was to obtain total energies accurate to 1 μHartree across the periodic table (i.e., better than a part in 10^{10} for U whose RLDA total energy is -28001.132325 Hartree); this goal was met. The only exact analytical results available to us are the total energies of one-electron atoms as given by solution of the Schrödinger equation (which are identical to orbital energy eigenvalues). We found that, in all cases, these energies were reproduced to the numerical accuracy of the computer for radial grid parameters similar to those used in our production runs. Thus, our basis for quoting the absolute numerical accuracies given here derives, first, from establishing the accuracy of one-electron calculations, and second, from observing consistency of the results of independent calculations, which was seen to improve systematically as the numerical grids were refined. The standard deviation σ of the total energies for the calculations among the various codes increase somewhat with the atomic number Z, but in no case does it exceed 0.5 μHartree; no two codes' results for total energy differ by more than 1μHartree in any case. The maximum eigenvalue deviations are 2 μHartree, and the maximum deviations for parts of the total energy (e.g., kinetic energy) are 8 μHartree.

11

A. Total energies and energy differences

As an example, we present the total energy and its decomposition as well as the eigenvalues for neutral Fe (Fe I) in Table II. Similar data is available for elements with Z=1-92 and their singly-charge cations via the World Wide Web [17].

Various quantities may be considered across the periodic table. Such plots have been made before, e.g., by Herman and Skillman [12] or Cowan [5] for empirically-corrected Hartree-Fock results.

The total energy calculated within the LDA and RLDA vary strongly with Z. To gain insight, we note that the leading behavior of the nonrelativistic total energy is given by Thomas-Fermi theory in the large Z limit [21]. The quantity $Z^{-7/3}E$ has much less variation than E itself, as shown in Fig. 1. The ScRLDA is seen to capture the majority of the energy difference between the LDA and the RLDA, indicating that the neglect of the (traceless) spin-orbit energy has been performed in a sensible way.

The Thomas-Fermi theory is shown as constant in Fig. 1. The first three leading terms in a series in $Z^{-1/3}$ of the exact total energy for the interacting many-electron large Z atom are known:

$$E(Z) = -(c_7 Z^{7/3} + c_6 Z^{6/3} + c_5 Z^{5/3} + ...)$$

with $c_7 = 0.768745$, $c_6 = -1/2$, and $c_5 = 0.2699$ Hartree [24]. These three terms are compared to our LDA results in Fig. 2. The agreement is remarkable given the simplicity of the LDA; indeed, the LDA apparently recovers these three terms. In order to obtain this agreement, the exchange-correlation terms have to be approximately correct. For U, the exchange-correlation energy is some 425 Hartree, but the $Z^{-1/3}$ expansion and our results differ by about 12 Hartree, i.e., less than 3% of the exchange-correlation energy. The Hartree-Fock results [8], also shown in Fig. 2, are quite similar to the LDA results computed here. Ref. [8] suggests that some of the oscillatory deviations shown in Fig. 2 may be due to the inadequacy of the three-term expression for $E(Z)$ rather than the Hartree-Fock calculation.

The spin-polarization energy is shown in Fig. 3. ¿From the point of view of atomic energies, the energies within the LSD track those within the LDA rather closely because the bulk of the energy comes from inner electrons which have nearly the same description in both theories. By construction, the theories give identical results for closed shell atoms. Nevertheless, the energy differences are large on the scale of chemical energies, ranging up to several electron volts (tenths of Hartrees). Aside from the very strong effects of shell structure, the trends which may be seen are: a peak in the spin polarization energy always occurs for half-filled shells; the spin-polarization energy is always largest for the first shell of a given orbital angular momentum (i.e., $1s$, $2p$, $3d$, and $4f$); and the spin-polarization energy increases with increasing angular momentum. However, the increase in spin-polarization energy with the orbital angular momentum is substantially, but not exclusively, accounted for by the larger number of electrons participating. The peak spin polarization energies occur for the elements H ($1s^1$), N ($2p^3$), Mn ($3d^5$), and Gd ($4f^7$), for which the spin polarization energies are 33.000, 111.783, 194.721, and 361.711 mHartree, respectively, or 33.000, 37.261, 38.944, and 51.673 mHartree per electron in the half-filled shell.

In Fig. 4, experimental ionization potentials [23] are compared to the total neutral-cation energy differences within the LDA and LSD. Both theories reproduce the important trends of shell structure out to large Z. The LSD captures a drop or shoulder in the curves in the middle of the $2p$, $3p$, and $4p$ series but not the $5p$, where relativistic effects move the drop to lower Z. The enhancement in the ionization potential at Gd in the middle of the $4f$ series is also captured by LSD. The RLDA does not systematically out-perform the LDA at large Z presumably because spin-polarization effects are omitted. Significant discrepancies between experiment and theory exist for the $3d$, $4d$, and $5d$ series in all approximations considered in this study.

B. Eigenvalues

The eigenvalues for all orbitals calculated within the LDA are shown in Fig. 5. The zero eigenvalue is the threshold for the continuum, i.e., zero kinetic energy and zero potential energy. For large Z, the core orbitals tend toward a hydrogenic form, i.e., the s, p, d, and f levels are degenerate for the same n. The valence orbitals always have a richer structure; they do not necessarily have the same ordering for different Z.

Because the four approximations give similar results, the energy differences are discussed below. The spin-orbit splitting is shown in Fig. 6 for p, d, and f levels. The splittings are seen to grow with a power law which is faster than the Z^4 of a hydrogenic orbital, e.g., $Z^{5.0}$ for the $2p$ level. When open shell effects are important, the comparison to experiment can be quite poor, as noted earlier by Herman and Skillman [13]. Multiplet effects which are more complicated than the spin-orbit splitting of a one-electron picture may dominate.

In Fig. 7, the difference between the LDA eigenvalue and the degeneracy-weighted average of the RLDA eigenvalues is shown. The trends are less regular than those in Fig. 6, because there is some opportunity for cancellation of errors. Specifically, the RLDA in a fixed potential leads to orbital contraction. For the outer orbitals, this implies more screening which will reduce or even outweigh the tendency to contract. Not surprisingly, the eigenvalue differences increase rapidly with Z, and decrease rapidly with n and ℓ. Fig. 8 offers a similar comparison between the ScRLDA and the RLDA. The differences are usually at least half an order of magnitude smaller than the previous comparison, indicating that the ScRLDA does indeed capture most of the relativistic effects.

The effects of spin polarization on the eigenvalues do not seem to follow a simple rule. The magnitude of the eigenvalue shift varies strongly with the spin-polarization, peaking for half-filled valence shells. The individual eigenvalues shift by an amount comparable to the spin-polarization energy shown in Fig. 2. The strongest polarization splitting does not necessarily belong to the valence eigenvalues. The $3d$, $4d$, and especially $4f$ orbitals are inside the atom; some of these outer core orbitals are more strongly affected in absolute

14

terms than the valence orbitals. There is no apparent systematic ℓ dependence in the shifts.

For open-shell atoms throughout the periodic table, the LSD eigenvalue associated with the majority spin lies below the minority spin eigenvalue in almost all cases. Perhaps it is surprising to note that the average eigenvalues for the core orbitals are shifted upward in the LSD. This may be seen for the case of Fe in Table II. To understand the flavor of these results, consider the case of Li. In the LDA, the $1s$ and $2s$ eigenvalues are -1.87856 and -0.10554 Hartree, respectively. In the LSD, the $2s$ eigenvalue is lowered to -0.11631 Hartree, as one might expect from the enhanced exchange-correlation potential. The $1s$ eigenvalues split, and become -1.87493 for the majority orbital and -1.86717 for the minority orbital. The majority $1s$ eigenvalue is lower than its minority counterpart as one might expect. Again, it is perhaps surprising that the eigenvalues themselves are both higher than in the LDA. The $1s$ orbital is largely inside the $2s$ orbital; for an estimate, it may be taken as completely inside the $2s$ orbital. The $2s$ orbital radius (inverse of the first inverse moment) drops from 2.828 bohr to 2.754 bohr. The shift in average radial position of the $2s$ orbital leads to a constant shift in Coulomb potential in its interior by $+9.5$ mHartree. The average $1s$ eigenvalue shift is $+7.5$ mHartree, a comparable value. Fig. 10 indicates that these shifts are larger for the inner orbitals. For the valence and outer core orbitals, the exchange-correlation splitting induced by LSD tends to outweigh this Coulomb effect. Deeper in the core, the Coulomb effect tends to be larger than the splitting, and both eigenvalues are shifted upward.

There are a few exceptions to the rule that the majority-spin orbital eigenvalues are below the minority-spin counterparts. However, even when there is an anomalous sign, usually the effect is less than 200μHartree and is limited to the $1s$ (or occasionally the $2s$) orbital. Copper is an exception to this rule, with the $2s$, $2p$, $3s$, and $3p$ minority spin orbitals lower than their majority spin counterparts by 1.0, 0.6, 1.0, and 0.4 mHartree, respectively.

IV. CONCLUSIONS

We have calculated the total energy and eigenvalues of neutral atoms and their singly charged cations across the periodic table ($Z = 1$-92) in four approximations: the local-density approximation (LDA), local-spin-density approximation (LSD), the relativistic LDA (RLDA), and the scalar-relativistic LDA (ScRLDA). We obtained agreement with 2 to 4 codes in each of these approximations to 1μHartree in the total energy; we also obtained similar agreement with the analytic solutions for the hydrogen atom using these codes. In this way, we hoped to achieve high reliability and high precision for the fundamental issue of the total energies of atoms within the local density approximation and its major variants. An overview has been presented in this work; all total energies and eigenvalues are available on the World Wide Web [17].

Here, we have presented the total energy in the large Z limit and have shown the LDA is in excellent agreement with an exact expansion in powers of $Z^{-1/3}$. The ScRLDA total energies are seen to give a very good account of the RLDA total energies despite having no spin-orbit term. Experimental ionization potentials are presented; the LSD gives the best agreement of the approximations presented across the periodic table; in particular it accounts for the energetics near half-filling. Selected trends across the periodic table have been presented to summarize the importance of the various effects on both eigenvalues and total energies.

The tables on the Web page may be used in several ways: as points of calibration for persons writing or using their own atomic codes, to generate excellent starting guesses in iterative atomic LDA programs, to estimate the magnitude of various effects (e.g., spin-orbit splitting) for particular elements which may aid researchers choosing an approximation in a molecular or solid-state calculation. Moreover, having a large data set on-line may aid studies of statistical or asymptotic characteristics of total energies and eigenvalues in the atomic central field problem of the local density approximation.

V. ACKNOWLEDGMENTS

REFERENCES

[1] J. F. Annett, Computational Materials Science **4**, 23 (1995).

[2] G. B. Bachelet, D. R. Hamann, and M. Schlüter, Phys. Rev. B **26**, 4199 (1982).

[3] H. A. Bethe and E. E. Salpeter, *Quantum Mechanics of One- and Two-Electron Atoms*, (Springer-Verlag, New York, 1957), p. 62.

[4] D. Ceperley and B. J. Alder, Phys. Rev. Lett. **45**, 4264 (1980).

[5] R. D. Cowan, *The Theory of Atomic Structure and Spectra*, (University of California, Berkeley, 1981), p. 237.

[6] J. P. Desclaux, Comp. Phys. Comm. **1**, 216 (1969); there is a factor of x^2 omitted on the right-hand side of Eq. (8) in this work.

[7] R. M. Dreizler and E. K. U. Gross, *Density Functional Theory,* (Sprinter-Verlag, Berlin, 1990), pp. 230ff.

[8] B.-G. Englert and J. Schwinger, Phys. Rev. A **32**, 47 (1985).

[9] P. Focher, A. Lastri, M. Covi, and G. B. Bachelet, Phys. Rev. B **44**, 8486 (1991).

[10] O. Gunnarsson and B. I. Lundqvist, Phys. Rev. B **13**, 4274 (1976).

[11] D. R. Hartree, *The Calculation of Atomic Structure,* (Permagon, New York, 1957).

[12] F. Herman and S. Skillman, *Atomic Structure Calculations,* (Prentice-Hall, Englewood Cliffs, NJ, 1963).

[13] Ref. [12], pp. 3-13.

[14] R. O. Jones and O. Gunnarsson, Rev. Mod. Phys. **61**, 689 (1989).

[15] D. D. Koelling and B. N. Harmon, J. Phys. C: Solid State Phys. **10**, 3107 (1977).

[16] W. Kohn and L. J. Sham, Phys. Rev. **140**, A1133 (1965).

[17] S. Kotochigova, Z. H. Levine, E. L. Shirley, M. D. Stiles, and C. W. Clark, http://math.nist.gov/DFTdata/ (1996).

[18] R. Latter, Phys. Rev. **99**, 5101 (1955).

[19] Z. H. Levine and J. W. Wilkins, J. Comp. Phys. **83**, 361 (1989).

[20] D. Liberman, J. T. Weber, and D. T. Cromer, Phys. Rev. **A137**, 27 (1965).

[21] E. H. Lieb and B. Simon, Phys. Rev. Lett. **31**, 681 (1973).

[22] A. H. MacDonald and S. H. Vosko, J. Phys. C: Solid State Phys. **12**, 2977 (1979).

[23] W. C. Martin and W. L. Wiese, in G. W. F. Drake, ed., *Atomic, Molecular, and Optical Physics Handbook,* (American Institute of Physics, New York, 1996), Chap. 10.

[24] J. D. Morgan III, in G. W. F. Drake, ed., *Atomic, Molecular, and Optical Physics Handbook,* (American Institute of Physics, New York, 1996), Chap. 22.

[25] J. P. Perdew and A. Zunger, Phys. Rev. B **23**, 5048 (1981).

[26] J. P. Perdew and Y. Wang, Phys. Rev. B **45**, 13244 (1992).

[27] A. K. Rajagopal and J. Callaway, Phys. Rev. B **7**, 1912 (1973).

[28] A. K. Rajagopal, J. Phys. C: Solid State Phys. **11**, L943 (1978).

[29] M. V. Ramana and A. K. Rajagopal, Phys. Rev. A **24**, 1689 (1981); Adv. Chem. Phys. **54**, 231 (1983).

[30] E. L. Shirley and R. M. Martin, Phys. Rev. B **47**, 15 404 (1993).

[31] J. C. Slater, Phys. Rev. **81**, 385 (1951).

[32] Y. Tal and M. Levy, Phys. Rev. A **23**, 408 (1981).

[33] E. P. Wigner, Phys. Rev. **46**, 1002 (1934); Trans. Faraday Soc. **34** 678 (1938).

[34] U. von Barth and L. Hedin, J. Phys. C: Solid State Phys. **5**, 1629 (1972).

[35] S. H. Vosko, L. Wilk, and M. Nusair, Can. J. Phys. **58**, 1200 (1980); S. H. Vosko and L. Wilk, Phys. Rev. B **22**, 3812 (1980).

[36] J. A. Bearden and A. F. Burr, Rev. Mod. Phys. **39**, 125 (1967); M. Cardona and L. Ley, Eds., Photoemission in Solids I: General Principles (Springer-Verlag, Berlin, 1978); J. C. Fuggle and N. Martensson, J. Electron Spectrosc. Relat. Phenom. **21**, 275 (1980); G. Williams, Brookhaven National Laboratory Informal Report 32953 (1996).

TABLE I. The parameters for the Vosko-Wilk-Nusair correlation functional.

		A	x_0	b	c
Paramagnetic	ε_c^P	0.0310907	-0.10498	3.72744	12.9352
Ferromagnetic	ε_c^F	0.01554535	-0.32500	7.06042	18.0578
Spin Stiffness	α_c	$-1/(6\pi^2)$	-0.00475840	1.13107	13.0045

TABLE II. Total energy and eigenvalues in Hartree for Fe I $3d^6 4s^2$ in four approximations; all digits shown are significant. For the LSD, two eigenvalues are given for each level; the lower energy corresponds to spin polarized in the majority-spin direction. For the RLDA, the two eigenvalues correspond to spin-orbit-split orbitals; the order is $p_{1/2}$ then $p_{3/2}$, and $d_{3/2}$ then $d_{5/2}$.

|	LDA	LSD	RLDA	ScRLDA
E_{tot}	-1261.093056	-1261.223291	-1269.229080	-1269.203563
T	1259.553429	1259.697871	1284.299765	1281.820878
E_{coul}	535.295832	535.733366	537.849537	537.639306
E_{enuc}	-3003.082484	-3003.635009	-3039.130268	3036.447136
E_{xc}	-52.859833	-53.019519	-52.248113	-52.216611
1s	-254.225505	-254.203661	-255.897914	-255.954644
		-254.202872		
2s	-29.564860	-29.577122	-29.990901	-29.999533
		-29.501754		
2p	-25.551766	-25.555535	-25.920510	-25.623699
		-25.498083	-25.464756	
3s	-3.360621	-3.415446	-3.428882	-3.429663
		-3.263810		
3p	-2.187523	-2.241326	-2.238116	-2.200495
		-2.093198	-2.181222	
3d	-0.295049	-0.343804	-0.289195	-0.285808
		-0.213912	-0.283569	
4s	-0.197978	-0.209988	-0.201119	-0.201138
		-0.182613		
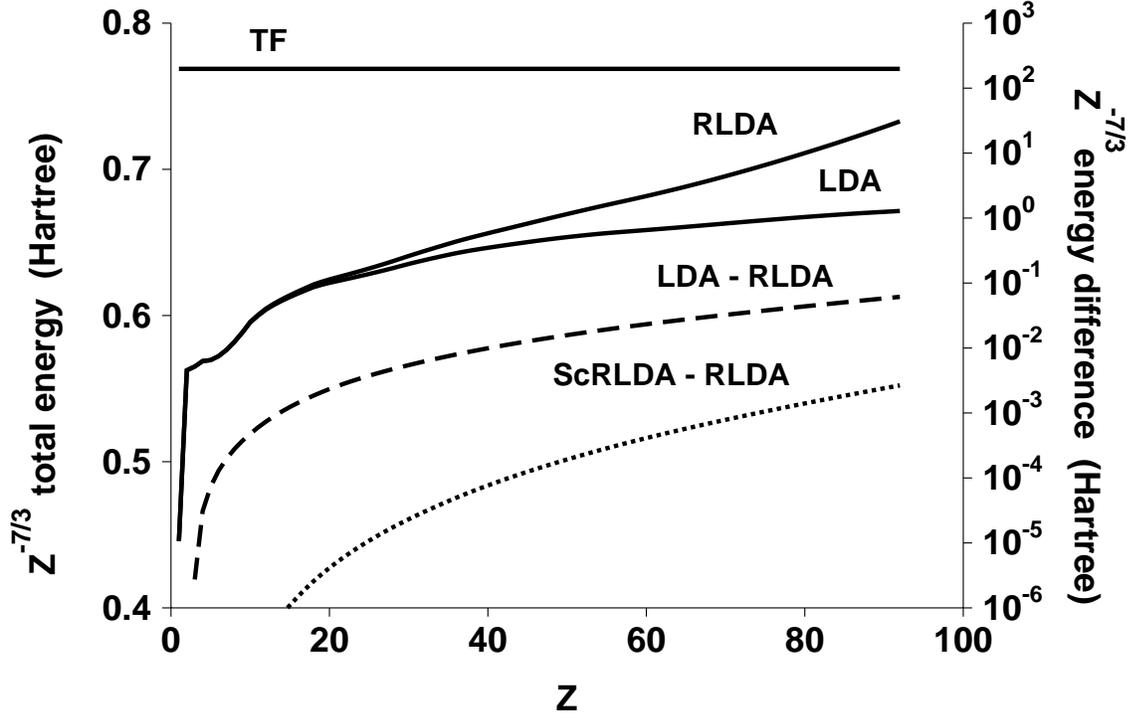
FIG. 1. The total energies of neutral atoms within the LDA, RLDA, and Thomas-Fermi theory, [32] scaled by a prefactor of $Z^{-7/3}$ (solid lines) are referred to the left axis. The Thomas-Fermi energy, $0.768745\, Z^{7/3}$ Hartree, is a constant on this graph. The differences in total energy LDA-RLDA (dashed line) and ScRLDA-RLDA (dotted line) are referred to the right axis.
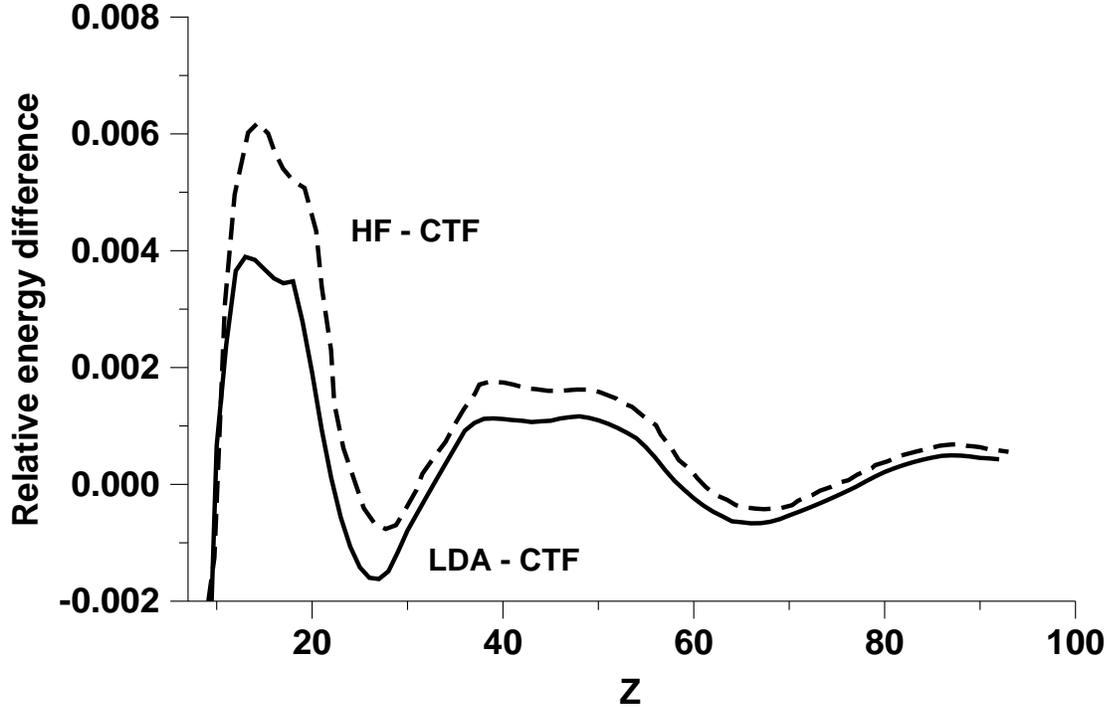
FIG. 2. The differences in total energy: the Thomas-Fermi with corrections in $Z^{6/3}$ and $Z^{5/3}$ (Ref. [8,24]) minus the LDA energy. The solid line gives the energy difference of the total LDA energy from the corrected Thomas-Fermi (CTF) theory (solid line) and the difference of the Hartree-Fock (HF) total energy from (CTF, dashed line, from Ref. [8]). The omitted values of the relative energy difference for the solid curve are: H 20.8%, He 3.7%, Li 2.4%, Be 1.4%, B-F, <1%.
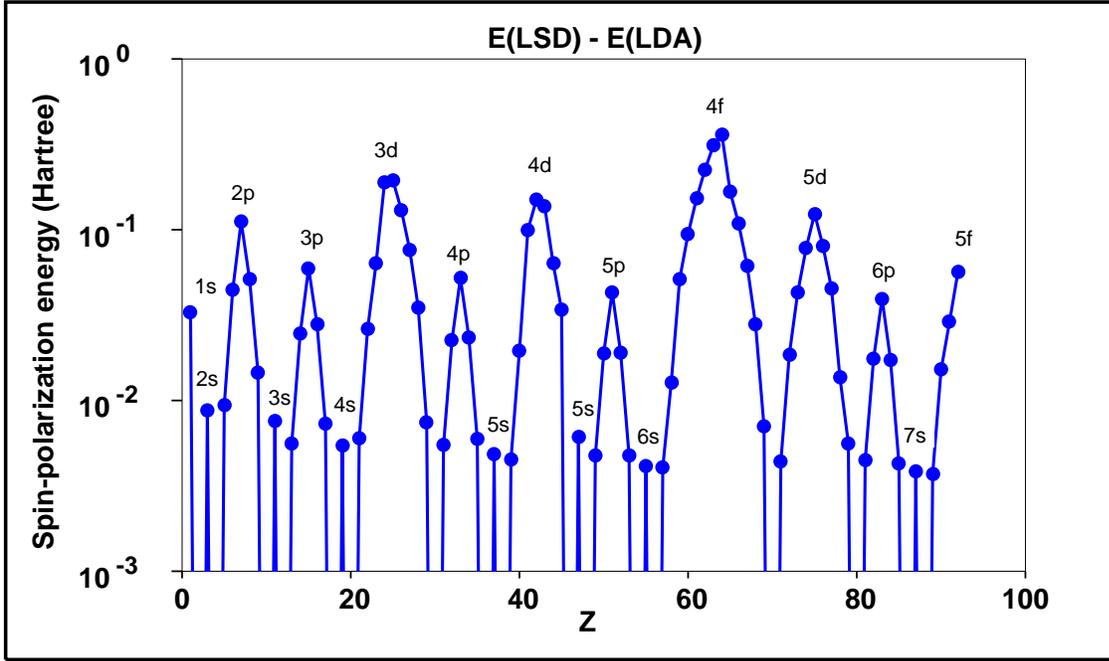
FIG. 3. The spin polarization energy for neutral atoms, i.e., the difference $E_{tot}^{LDA} - E_{tot}^{LSD}$. The labels refer to the principal partially filled shell for a given Z. The spin polarization is strictly zero for the closed shell atoms (i.e., He, Be, Ne, Mg, Ar, Ca, Cu, Kr, Sr, Pd, Cd, Xe, Ba, Yb, Hg, Rn, and Ra) The maximum spin-polarization energy occurs for Gd, which has a half-filled $4f$ shell. The $5s$ shell fills twice, first for Rb and Sr before the $4d$ series and second for Ag and Cd afterwards.
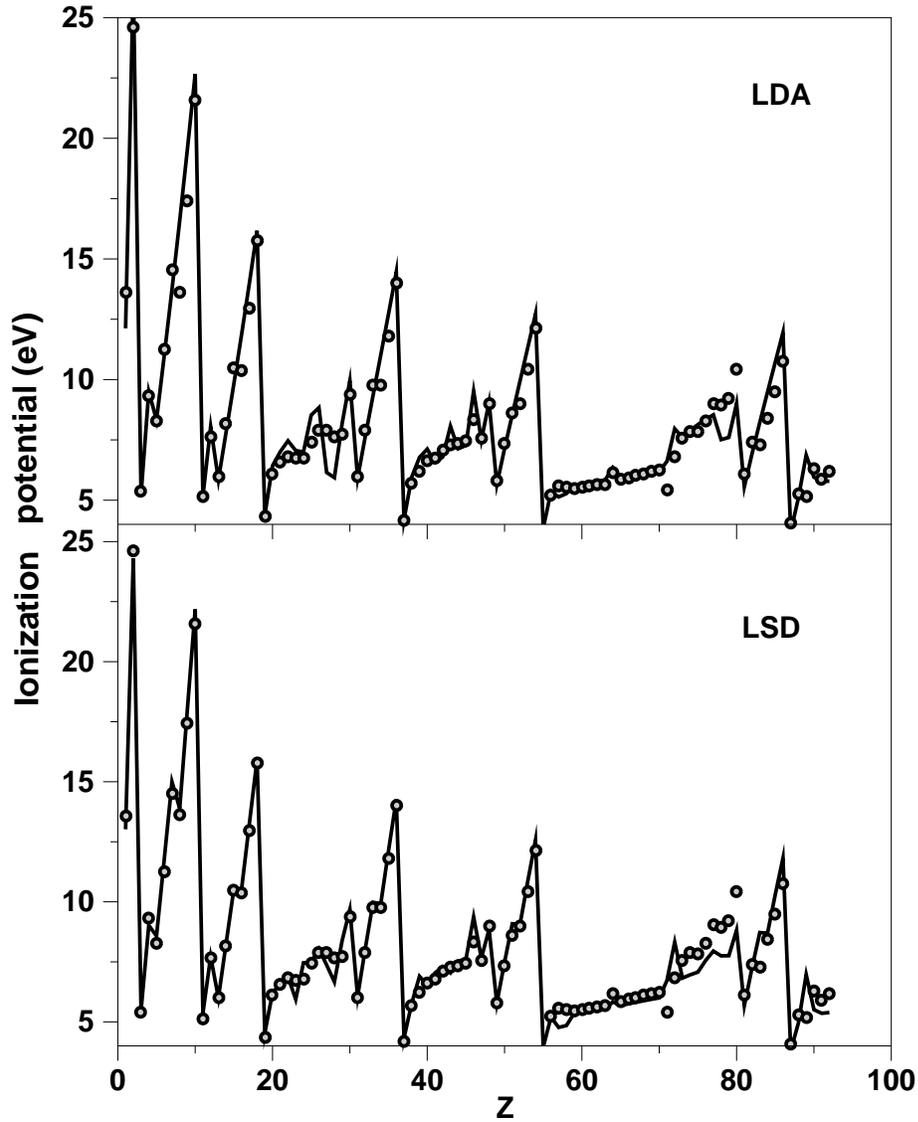
FIG. 4. Experimental ionization potentials [23] (open circles) are compared to the total energy differences within the LDA (solid line – upper panel) and LSD (solid line – lower panel). The RLDA is shown in an inset; up to medium Z the differences from the LDA cannot be resolved on the plot. Elements of the V_B series (which have a half-filled valence p shell) are indicated on the lower panel.
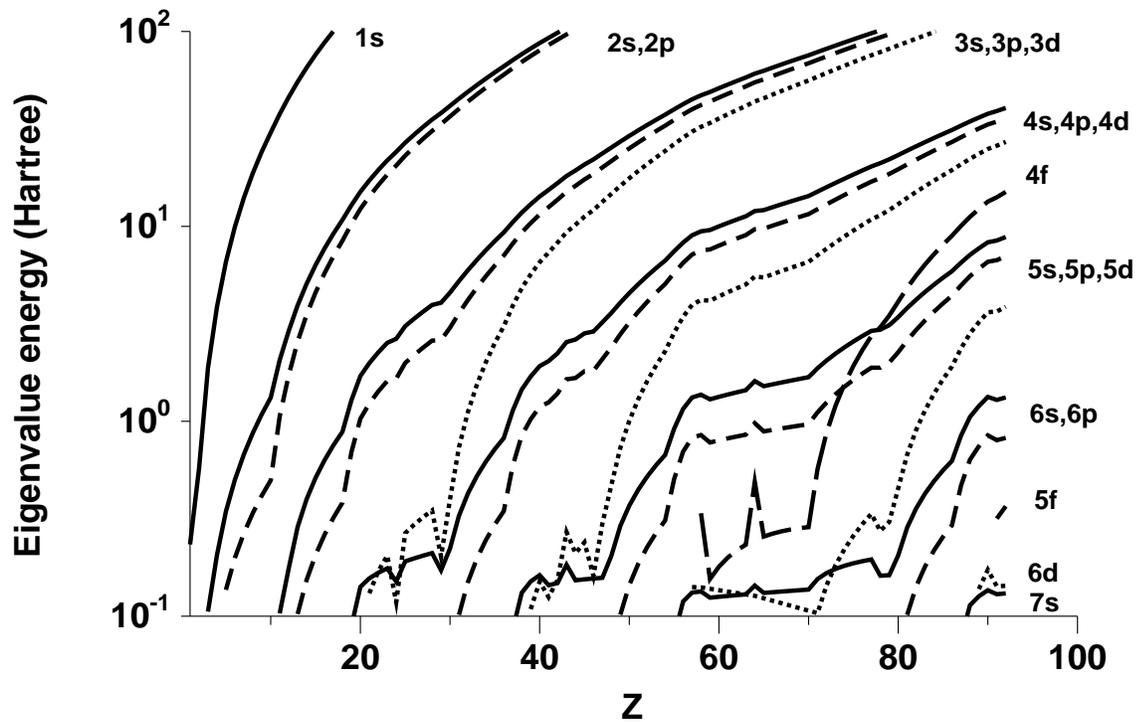
FIG. 5. Eigenvalues in the LDA; negative sign omitted. The solid lines are s levels, the short-dashed lines are p levels, the dotted lines are d levels and the long-dashed lines are f levels.
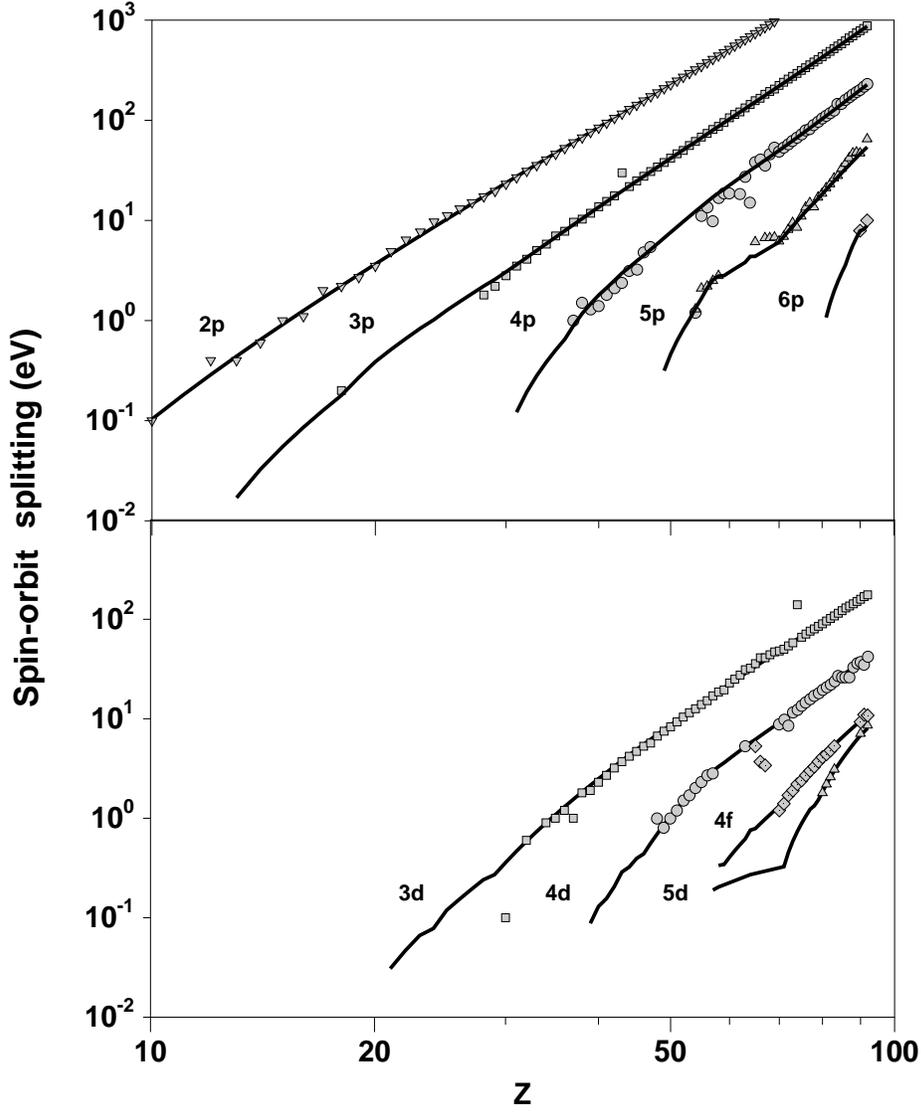
FIG. 6. Spin-orbit splittings i.e., the eigenvalue difference of $p_{3/2}-p_{1/2}$, $d_{5/2}-d_{3/2}$, or $f_{7/2}-f_{5/2}$ within the RLDA and by experiment (differences in x-ray absorption thresholds) [36] for various p levels (upper figure) and d and f levels (lower graph).
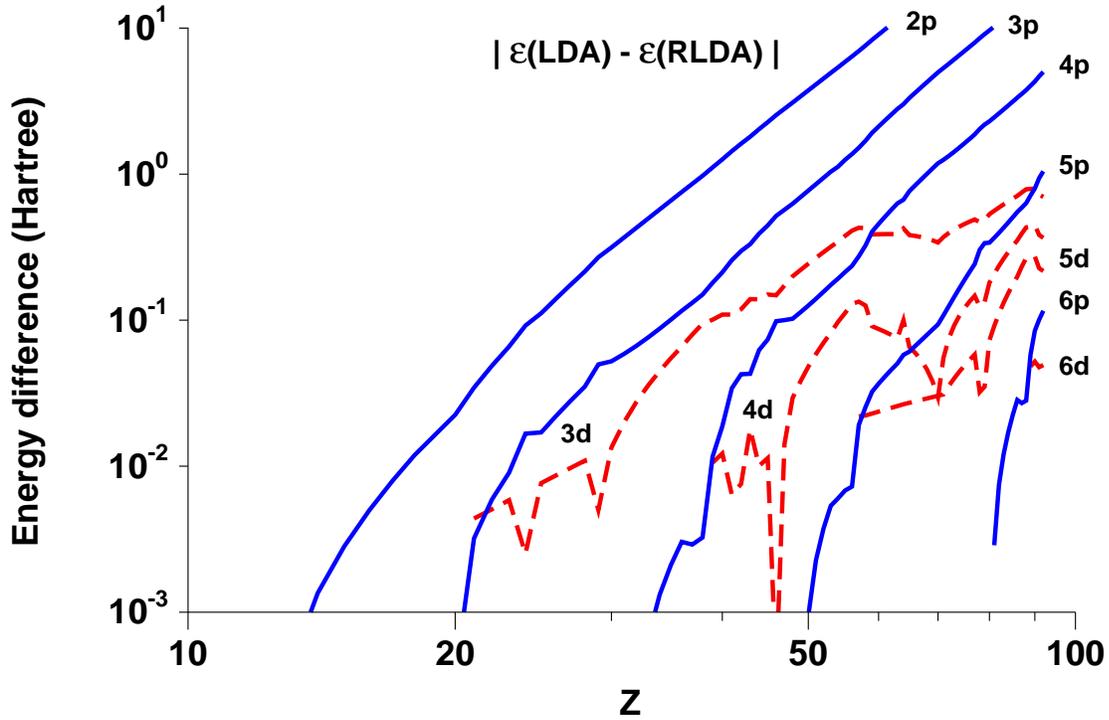
FIG. 7. Differences of eigenvalues between the RLDA and the LDA for selected levels. Here, the RLDA eigenvalues are given a population-weighted average over the two spin-orbit split pairs. The effect of relativity increases with Z, but decreases with quantum numbers n and ℓ.
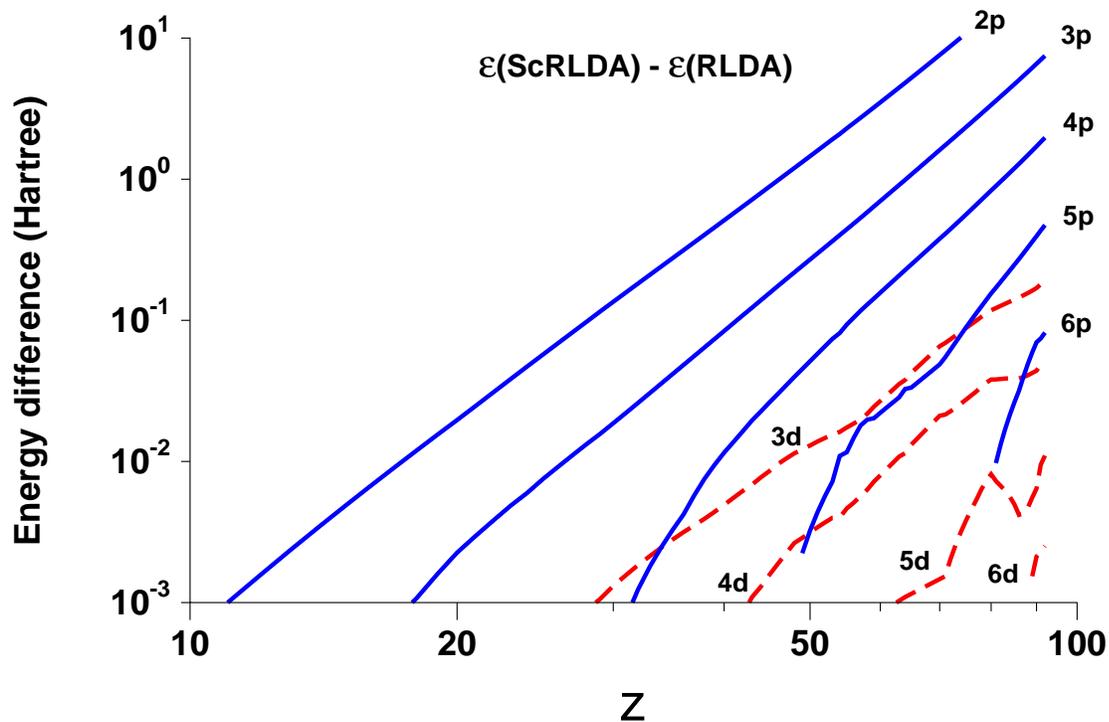
FIG. 8. Differences of eigenvalues between the ScRLDA and RLDA for selected levels. As in Fig. 7, the RLDA is the population-weighted average of the two spin-orbit split pairs. The ScRLDA is at least half and order of magnitude than the LDA for obtaining the averaged RLDA eigenvalues for $Z \geq 30$.